JOM, Vol. 67, No. 9, 2015
DOI: 10.1007/s11837-015-1483-8

High-Zinc Recovery from Residues by Sulfate Roasting and Water Leaching

MING HU,[1] BING PENG,[1,2,3,4] LI-YUAN CHAI,[1,2] YAN-CHUN LI,[1] NING PENG,[1] YING-ZHEN YUAN,[1] and DONG CHEN[1]

1.—Institute of Environmental Science and Engineering, School of Metallurgy and Environment, Central South University, Changsha 410083, Hunan, People's Republic of China. 2.—Chinese National Engineering Research Center for Control & Treatment of Heavy Metal Pollution, Changsha 410083, Hunan, People's Republic of China. 3.—e-mail: bingcsu@hotmail.com. 4.—e-mail: pb1956@yahoo.cn

An integrated process for the recovery of zinc that is generated from zinc hydrometallurgy in residues was developed. A mixture of residue and ferric sulfate was first roasted to transform the various forms of zinc in the residue, such as ferrite, oxide, sulfide, and silicate, into zinc sulfate. Next, water leaching was conducted to extract the zinc while the iron remained in the residue as ferric oxide. The effects of the roasting and leaching parameters on zinc recovery were investigated. A maximum zinc recovery rate of 90.9% was achieved for a mixture with a ferric sulfate/residue weight ratio of 0.05 when roasting at 640°C for 30 min before leaching with water at room temperature for 20 min using a liquid/solid ratio of 10. Only 0.13% of the iron was dissolved in the water. Thus, the leaching liquor could be directly returned for zinc smelting.

INTRODUCTION

Currently, more than 85% of the metal zinc on Earth is produced using the conventional hydrometallurgical approach, which includes oxidative roasting, acid leaching, purification, and electrowinning processes (RLPE).[1,2] During these processes, large amounts of residue containing zinc ferrite are produced and accumulate, resulting in loss of metals, increased need for a landfill, and severe environmental pollution.

Pyrometallurgical and hydrometallurgical processes are generally used to treat this residue. In pyrometallurgical processes, industrial Waelz and Ausmelt furnaces are used to recover metals. However, these processes consume large amounts of power and coal and require a high operating temperature (1100–1300°C) to decompose zinc ferrite. Furthermore, large amounts of secondary residues with high iron contents are generated.[3] These shortcomings also occur in other pyrometallurgical methods, such as roasting with Na_2CO_3 and Na_2S.[4–6] To overcome these disadvantages, a new reduction roasting-magnetization technology was developed in which zinc ferrite can be transformed into zinc oxide and magnetic ferric oxide under a reducing atmosphere at a temperature of approximately 750°C.[7–9] However, the reducing atmosphere is difficult to control in the roasting process and results in a lower zinc ferrite composition. Given these challenges, a series of hydrometallurgical processes were studied, such as high-pressure acid leaching, two-stage acid leaching, microwave caustic leaching, di-2-ethylhexyl phosphoric acid (D2EHPA) leaching, and the use of various acidic or highly alkaline solutions.[10–18] In addition, several other hydrometallurgical processes were developed, including the use of ammoniac solutions and chloride leaching.[1,19–23] A high zinc-leaching rate was achieved during these processes. However, severe leaching conditions, such as a high temperature (90–95°C) and high acidity (200–250 g/L), were required for the decomposition of zinc ferrite. In addition, the leaching rate of iron significantly increased under the enhanced leaching conditions. Thus, complicated upstream precipitation processes are required for removing iron before electrowinning. Moreover, long-term operation and high costs make these techniques unsuitable for industrial production. Therefore, an efficient, convenient, and

(Published online June 16, 2015)

cost-effective process is highly desirable for recovering zinc from zinc residues.

This article focuses on the recovery of zinc from residues by sulfate roasting and subsequent water leaching. During the roasting stage, the various forms of zinc in the residues, including zinc oxide, sulfide, sulfate, silicate, and ferrite, are transformed into soluble zinc sulfate and iron is transformed into insoluble ferric oxide. Then, simple water leaching is used to recover the zinc from the roasted residues. During this process, the iron remaining in the leached residues is successfully separated from zinc, and the leachate is used directly to recover the zinc without complicated iron precipitation processes. Moreover, this newly developed process employs a lower roasting temperature and allows a simpler overall process than traditional pyrometallurgical and hydrometallurgical processes.

EXPERIMENTAL

Materials and Analyses

The residues used in this study were obtained from a hydrometallurgical zinc plant located in Hunan Province, China, and consisted of mixtures of zinc leaching and jarosite ($KFe_3(SO_4)_2(OH)_6$) residues. The samples were dried at 105°C for 24 h before grinding and sieved to yield a particle size of less than 74 μm before performing the experiments. The elemental composition of the residue was determined by using an x-ray fluorescence spectrometer (XRF) (Table I). The crystalline phases of the samples were investigated by using x-ray powder diffraction (TTR-III; Rigaku Corporation, Tokyo, Japan) on two scales using CuKa radiation (k = 1.5406 A, 50 kV, and 100 mA) at as scanning rate of 10/min and ranging from 10° to 8°. The XRF results indicated that this sample was composed of Zn-9.6%, Fe-30.8%, S-8.6%, O-38.7%, Si-3.3%, Cu-1.2%, and Pb-1.3%. The XRD (Fig. 1) pattern indicated that the residue was mainly composed of zinc ferrite ($ZnFe_2O_4$), plumbojarosite ($PbFe_6(SO_4)_4(OH)_{12}$), and natrojarosite ($NaFe_3(SO_4)_2(OH)_6$). Most of the zinc in the residues was present as zinc ferrite (59.6%), with zinc oxide, zinc silicate, and zinc sulfate as minor components. The zinc distribution is shown in Table II. The morphological changes were detected by using a scanning electron microscope (SEM; JSM-6360LV; JEOL Ltd., Tokyo, Japan). The particle size distribution was measured using conventional wet screening and a laser particle size analyzer (LPSA) (MICRO-PLUS; Malvern Instruments Ltd., Malvern, U.K.). A simultaneous thermogravimetric-differential scanning calorimetry investigation was carried out using a thermal analyzer (NETZSCH STA 449C; NETZSCH Pumps North America LLC, Exton, PA). Finally, ethylenediaminetetraacetic acid titration methods were used to quantitatively analyze zinc sulfate, zinc ferrite, and total zinc to evaluate the experimental results.

Sulfate Roasting

An appropriate amount of ferric sulfate was mixed with 20 g of residue using a mortar and pestle. The mixture was placed into a corundum crucible, covered, and roasted in a high-temperature furnace (HTK40-18) at approximately 640°C. After roasting, the residue mixture was removed from the apparatus and cooled to room temperature. Finally, the roasted products were weighed, ground, and stored in a tightly closed jar until analysis.

The influences of roasting parameters, such as temperature, duration, and ferric sulfate dose, were studied. The decomposition rate of zinc ferrite and the proportion of zinc sulfate were used to evaluate the roasting effects and were calculated using the following equation:

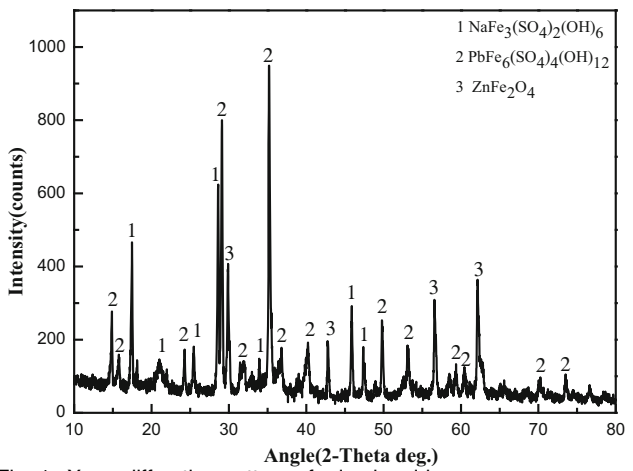

Fig. 1. X-ray diffraction pattern of mixed residues.

Table I. Chemical composition of mixed residue determined using XRF

Elements	Content (wt.%)	Elements	Content (wt.%)	Elements	Content (wt.%)
Fe	30.77	Na	1.17	Mg	0.10
O	38.70	Cu	1.15	K	0.628
Zn	9.62	Al	0.63	Ba	0.044
S	8.59	As	0.79	Sr	0.006
Si	3.34	Ca	0.65	Cd	0.080
Pb	1.31	Mn	0.319	Sb	0.075

Table II. Analysis of the phases of zinc in the mixed residues

Phase composition	$ZnSO_4$	ZnO	$ZnSiO_3$	ZnS	$ZnFe_2O_4$	Others
Zn content (wt.%)	1.29	1.4	0.49	0.62	5.73	0.02
Phase occupation ratio (%)	13.41	15.28	5.09	6.44	59.56	0.22

$$\alpha = \frac{C_0 - C_r}{C_0} \times 100\% \quad (1)$$

$$\beta = \frac{C_s}{C_t} \times 100\% \quad (2)$$

where α is the decomposition rate of zinc ferrite, and C_0 and C_r represent the zinc ferrite contents in the initial and roasted residues, g/L, respectively. In addition, β is the proportion of zinc sulfate, C_s represents the zinc sulfate content in the roasted residue, g/L; and C_t is the total zinc content in the roasted residue, g/L.

Water Leaching

Water leaching was conducted to selectively separate the zinc sulfate from the residue. The leaching process was carried out using an agitator with a controlled leaching temperature. The leaching parameters, namely temperature, time, and liquid/solid ratio, were studied. The recovery rate of zinc and iron was used to evaluate the effects of water leaching and determined as follows:

$$\gamma = \frac{C_l}{C_t} \times 100\% \quad (3)$$

where γ is the recovery rate of zinc or iron; C_l is the zinc or iron content in the leaching liquid, g/L; and C_t is the total zinc or iron content in the roasted residue, g/L.

Reaction Mechanism

During the roasting process, a series of reactions occurred in the mixed residues, as demonstrated by the differential thermal and derivative thermogravimetric analysis (DTA-DTG) chart and thermodynamic data. Figure 2 shows that the dehydration of residues was completed at approximately 250°C.[24,25] Then, the jarosite in the residues decomposed to ferric sulfate and ferric oxide as its lattice was destroyed at approximately 450°C.[25] Thus, large amounts of ferric sulfate were produced from jarosite decomposition, which would reduce the addition of artificial ferric sulfate in subsequent experiments. Finally, as the temperature increased, the DTA-DTG chart showed that the last endothermic peak occurred at approximately 640°C. However, this DTA-DTG chart differed from that of pure ferric sulfate (Fig. 3) reported in the literature, which potentially occurred because the ferric sulfate

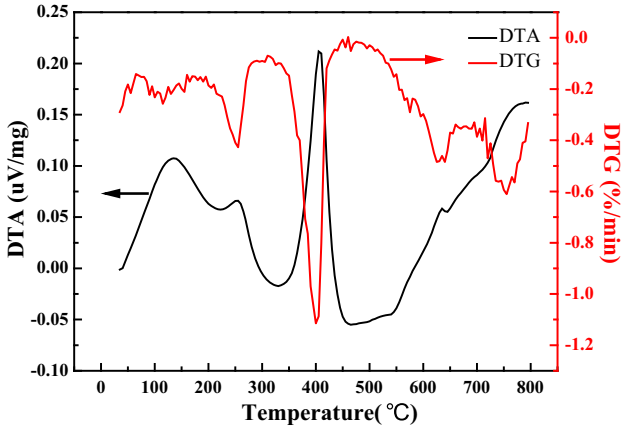

Fig. 2. DTA-DTG chart for the mixed residue.

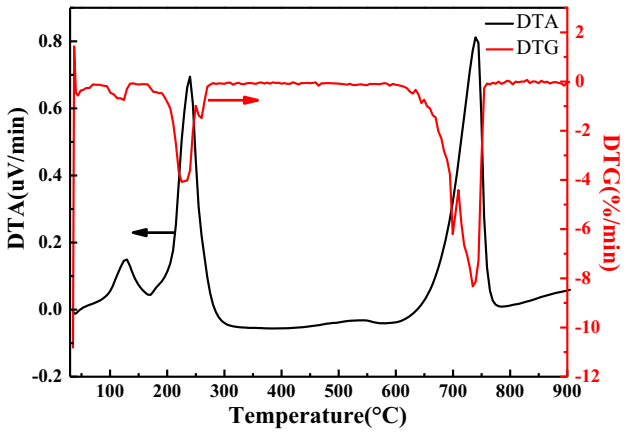

Fig. 3. DTA-DTG chart for pure ferric sulfate.

produced from jarosite decomposition was further decomposed to form sulfur trioxide and ferric oxide.[24,25] The gaseous product immediately reacted with various forms of zinc, including zinc ferrite, oxide, and silicate.[26,27] This immediate reaction likely caused the various forms of zinc in the residue to transform into zinc sulfate after roasting. These sulfating reactions are potentially supported by the Gibbs energy, which is shown in Fig. 4. The Gibbs energy reveals the standard free energy changes of these reactions at temperatures of 600–750°C. The results indicated that these sulfating reactions could occur between 600°C and 750°C because their Gibbs energy is always less than zero. The decomposition and sulfation reactions can be written as follows:

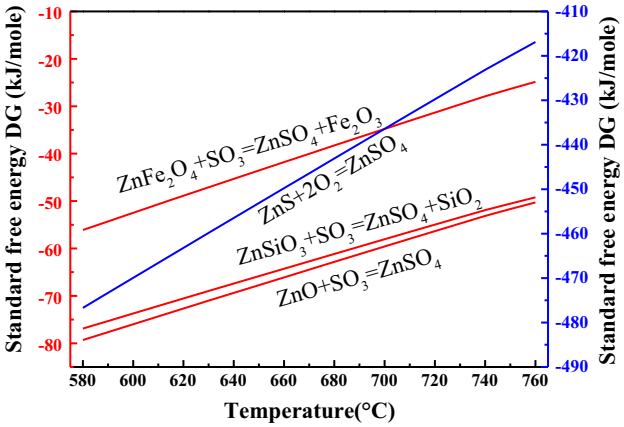

Fig. 4. Standard free energy changes for sulfation reactions across a temperature range of 600–750°C.

$$MFe_x(SO_4)_y(OH)_z \rightarrow MSO_4 + Fe_2O_3 + Fe_2(SO_4)_3 + H_2O \quad (4)$$

$$Fe_2(SO_4)_3 \rightarrow Fe_2O_3 + 3SO_3 \quad (5)$$

$$ZnFe_2O_4 + SO_3 \rightarrow ZnSO_4 + Fe_2O_3 \quad (6)$$

$$ZnSiO_3 + SO_3 \rightarrow ZnSO_4 + SiO_2 \quad (7)$$

$$ZnO + SO_3 \rightarrow ZnSO_4 \quad (8)$$

$$ZnS + 2O_2 \rightarrow ZnSO_4 \quad (9)$$

where *M* represents a metal, such as Na, K, or Pb.

Based on these mechanisms, the temperature should be maintained at approximately 640°C to produce sulfur trioxide through the decomposition of zinc ferrite in the residues and recover zinc from the residues.

RESULTS AND DISSCUSSION

Effects of Roasting Temperature

Among the factors influencing the roasting process, the roasting temperature was the first parameter to be varied while maintaining the reaction duration at 0.5 h. The influences of the roasting temperature on zinc ferrite decomposition and the proportion of zinc sulfate are represented in Fig. 5. As shown in Fig. 5a, the decomposition rate of zinc ferrite and the proportion of zinc sulfate increased with temperature up to 640°C. The decomposition rate reached its maximum of 79.4% when the temperature was 640°C and then decreased to 62.7% as the temperature continued to increase. These changes in the decomposition rate occurred because the ferric sulfate that was produced by the decomposition of jarosite was easily transformed to sulfur trioxide at higher temperatures and because the speed of the reaction of sulfur trioxide with zinc ferrite increased under high-temperature conditions in the residues. However, sulfur trioxide also easily escaped at higher temperatures and reduced the occurrence of the subsequent transformation reactions. Thus, the decomposition rate of zinc ferrite and the proportion of zinc sulfate decreased when the temperature exceeded 640°C. Considering that sulfur trioxide could react with zinc ferrite quickly, it was concluded that 640°C was an appropriate roasting temperature.

Effects of Roasting Time

The roasting time significantly influences the decomposition of zinc ferrite and the proportion of zinc sulfate. The influences of roasting time at a roasting temperature of 640°C are shown in Fig. 5b. Figure 5b shows that the decomposition rate of zinc ferrite and the proportion of zinc sulfate were maximized when a roasting time of 30 min was used. These results indicated that the rate of the transformation of ferric sulfate into sulfur trioxide and the reaction of sulfur trioxide with zinc ferrite were rapid under these conditions (640°C). Thus, a roasting time of 30 min was sufficient for completing these reactions. This conclusion was confirmed by the phase transformation of the residues. The XRD (Fig. 6) patterns revealed that the iron in the residues (640°C, 0.5 h) was in the form of ferric oxide rather than ferric sulfate, which indicated that the ferric sulfate produced from jarosite was completely transformed into sulfur trioxide and ferric oxide. In addition, as shown in Fig. 6b, the intensities of the characteristic peaks of zinc ferrite significantly decreased, and a new characteristic peak of zinc sulfate appeared. These phase transformations of the roasted residues indicated that the zinc ferrite was effectively transformed into zinc sulfate by reacting with the sulfur trioxide that was produced from the residues within 30 min. However, when the roasting time exceeded 30 min, the decomposition rate of zinc ferrite and the proportion of zinc sulfate in the total zinc decreased, potentially because the zinc sulfate decomposed into zinc oxide, and zinc ferrite was formed from the reaction of zinc oxide with ferric oxide. Although further investigations are necessary to confirm this hypothesis, it was considered that 30 min is an appropriate roasting time in this study.

Effects of Ferric Sulfate Content

The experiments showed that the ferric sulfate content plays an important role in zinc recovery. More ferric sulfate results in more sulfur trioxide, which can react with zinc ferrite. The ferric sulfate produced by the decomposition of jarosite could be insufficient for effectively decomposing zinc ferrite.

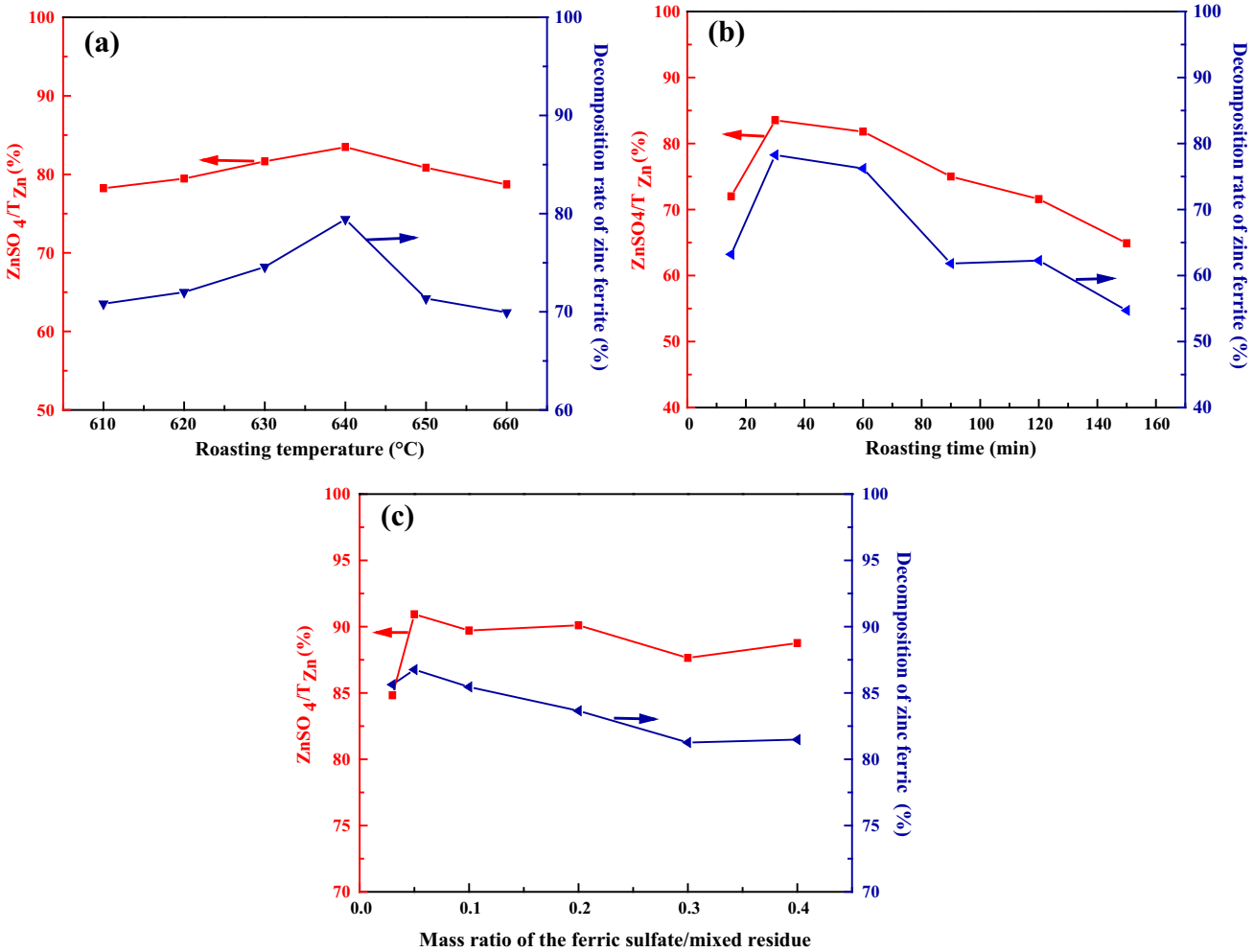

Fig. 5. The effects of roasting parameters for zinc recovery: (a) roasting temperature, (b) roasting time, and (c) mass ratio of the ferric sulfate/mixed residue.

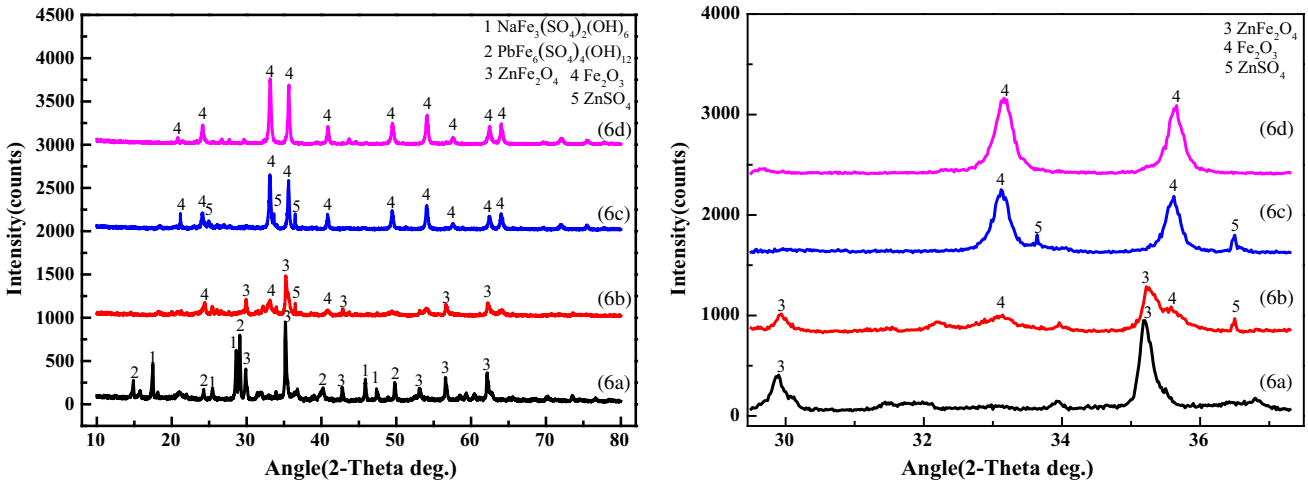

Fig. 6. X-ray diffraction pattern of residues under different conditions: (a) mixed residues, (b) mixed residues at 640°C for 0.5 h, (c) mixed residues at 640°C for 0.5 h and with a ferric sulfate/residue ratio of 0.05, and (d) roasted residues after water leaching.

Therefore, additional ferric sulfate was added in the experiments, and a series of experiments were completed using the determined appropriate roasting temperature (640°C) and time (0.5 h). The results shown in Fig. 5c indicate that the decomposition rate of zinc ferrite increased sharply before reaching its

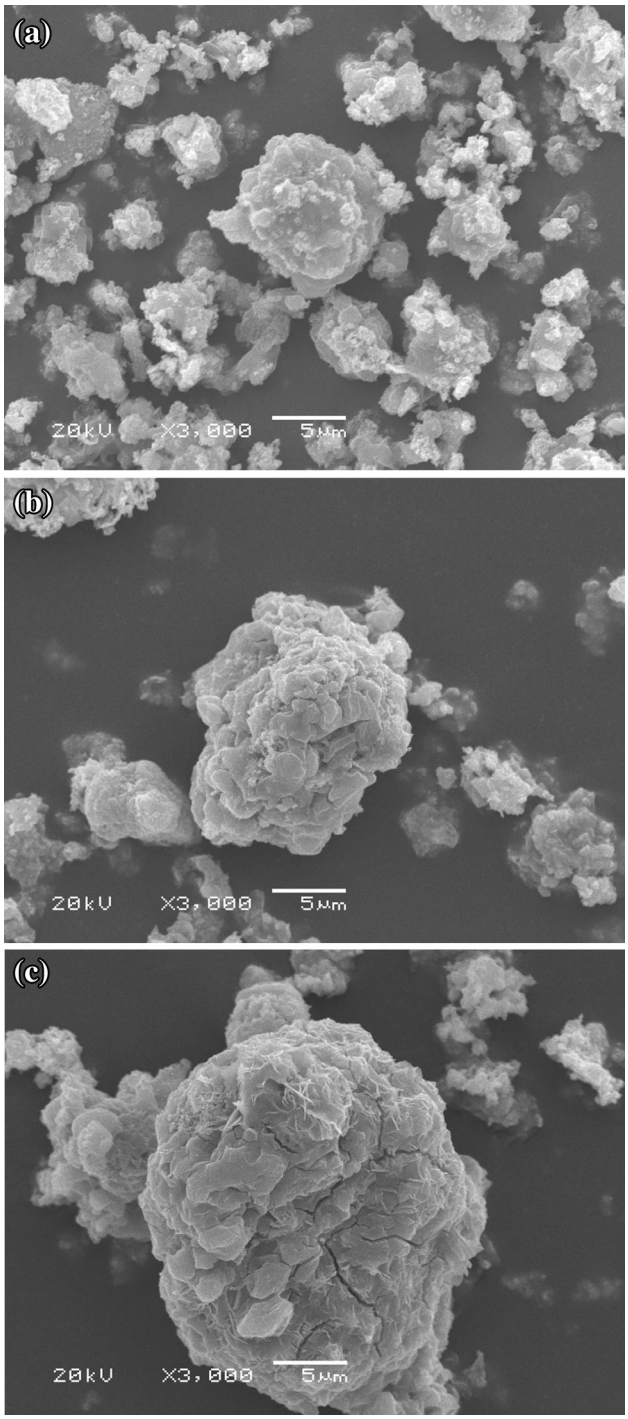

Fig. 7. SEM images of residues under different conditions: (a) residues before roasting, (b) the residues after roasting at 640°C for 30 min and with a ferric sulfate/residue ratio of 0.05, and (c) the residues after roasting at 640°C for 30 min and with a ferric sulfate/residue ratio of 0.3.

maximum rate of 86.8% when the mass ratio of the ferric sulfate/mixed residue was 0.05. In addition, the ratio of the ferric sulfate/mixed residue increased by nearly 7% relative to the results without additional ferric sulfate. The proportion of zinc sulfate showed a similar trend and reached a maximum value of

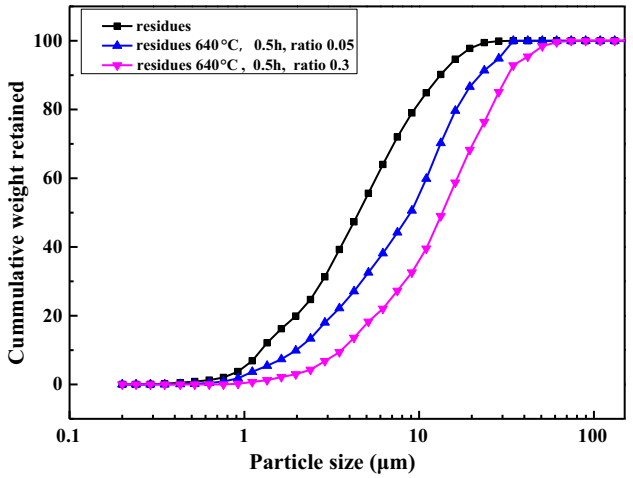

Fig. 8. Particle size distribution of the residues as determined by the LPSA technique.

90.9%. However, after the ratio exceeded 0.05, the decomposition rate of zinc ferrite and the proportion of the zinc sulfate decreased rather than increased with increasing amount of ferric sulfate. This result could be explained by the morphological changes in the mixed residue after roasting and was examined by SEM (Fig. 7). As shown in Fig. 7, the residues were sintered after roasting, which resulted in the removal of chemical or crystalline water from the samples. After roasting, the zinc ferrite was unable to completely contact the sulfur trioxide due to the partially sintered particle surfaces not accessible for reaction anymore. Meanwhile, the average particle size sharply increased as the amount of ferric sulfate increased. Figure 8 supports this assumption and shows that the d_{50} of the residues increased from 4.52 μm to 9.06 μm and 13.8 μm after roasting under the abovementioned conditions, which demonstrated that the sintering between the samples became more pronounced and prevented further decomposition of the zinc ferrite. This decomposition contributed to the decreased decomposition rate of zinc ferrite while increasing the amount of ferric sulfate. Thus, a ferric sulfate/residue ratio of 0.05 was considered as an optimal parameter for the decomposition of zinc ferrite.

Finally, the phase analysis of zinc was conducted again using the samples produced under the determined optimum roasting conditions (640°C, 0.5 h, and a ferric sulfate/residue ratio of 0.05). The results are shown in Table III. Zinc oxide and zinc sulfide were not detected in the samples, and the zinc ferrite and zinc silicate contents significantly decreased. Equations 6–9 could occur when the zinc sulfate content in the mixed residue is high.

Phase Transformations During Sulfate Roasting Process

XRD analyses were performed to identify the phase transformation that occurs during sulfate

Table III. Analysis of the phases of zinc in the roasted and mixed residues

Phase composition	$ZnSO_4$	ZnO	$ZnSiO_3$	ZnS	$ZnFe_2O_4$	Others
Zn content (wt.%)	10.23	0	0.18	0	0.81	0.03
Phase occupation ratio (%)	90.93	0	1.60	0	7.20	0.27

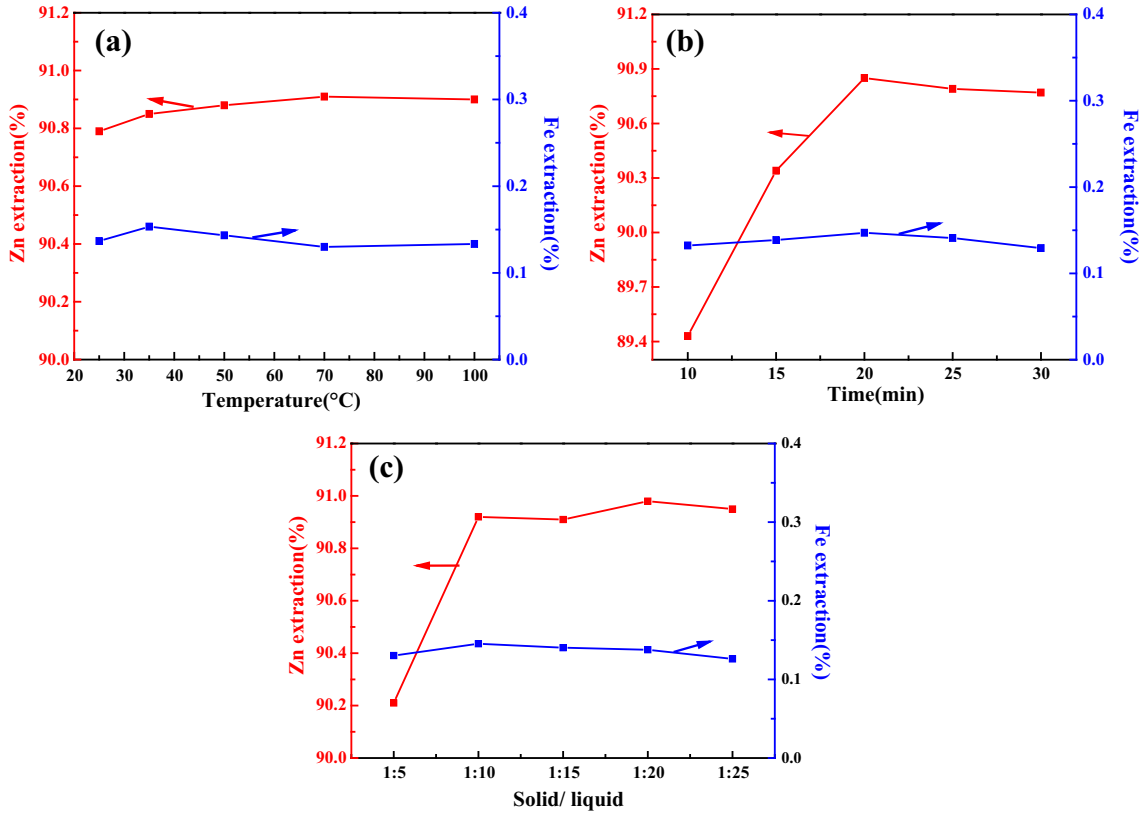

Fig. 9. The effects of leaching parameters for zinc recovery: (a) temperature, (b) time, and (c) solid/liquid.

roasting, as shown in Fig. 6a. The main phase in the residues was zinc ferrite. When the residues without ferric sulfate were subjected to temperatures of 640°C for 0.5 h, as shown in Fig. 6b, the intensities of the characteristic peaks of zinc ferrite significantly decreased. In addition, a new characteristic peak of ferric oxide and zinc sulfate appeared, which indicated that the zinc ferrite was transformed to zinc sulfate and ferric oxide. However, zinc ferrite still existed in the residues because the ferric sulfate that was produced from the decomposition of jarosite was not sufficient for completely transforming the zinc ferrite. When appropriate ferric sulfate (a ferric sulfate/residue ratio of 0.05) was added and then the mixed samples were roasted at 640°C for 0.5 h, the characteristic peaks of zinc ferrite disappeared completely. Simultaneously, the intensities of the characteristic peaks of zinc sulfate and ferric oxide significantly increased, as shown in Fig. 6c. This change indicated that the zinc ferrite in the mixed residues was further transformed into zinc sulfate. This finding agrees well with previous experimental results. Furthermore, the zinc in the roasted residues existed as soluble zinc sulfate rather than as zinc ferrite, and iron existed as insoluble ferric oxide. This effective separation of zinc and iron explained the extremely high recovery rate of zinc without simultaneous iron dissolution after subsequent residue leaching.

Effects of Leaching Parameters on Zinc Recovery

To obtain a high zinc recovery rate, the residue was subjected to leaching with water after roasting. The effects of the leaching temperature, leaching time, and liquid/solid ratio on the recovery of zinc were investigated. Figure 9a clearly shows that the zinc

and iron recovery rates were 90.8% and 0.13%, respectively, at 25°C. When the leaching temperature increased, the recovery rates hardly changed, which indicated that the leaching temperature had no significant effect in the investigated temperature range. Therefore, the optimum leaching temperature was determined to be at 25°C and was subsequently used in this study. However, the metal extraction can be improved by prolonging the leaching periods. Moreover, the liquid/solid ratio is an important parameter in the actual production process. In this study, the effects of the leaching time and liquid/solid ratio on the recovery rate of zinc were studied. As shown in Fig. 9b and c, the zinc recovery rate quickly peaked, but the iron concentration remained low and did not change with increasing leaching time and liquid/solid ratio. This result occurred because of the high water solubility of the zinc sulfate and the insolubility of the ferric oxide. A leaching time of 20 min and a liquid/solid ratio of 10 were determined to be suitable for achieving the high zinc recovery goal. Practically, relatively short leaching periods and small liquid/solid ratios are more economical. The optimum parameters observed in this study were 25°C, 20 min, and a liquid/solid ratio of 10.

Phase Transformation of Mixed Residues After Water Leaching

As shown in Fig. 6d, after water leaching under the determined optimum conditions (25°C, 20 min, liquid/solid ratio of 10), the intensities of the characteristic peaks of zinc sulfate decreased and iron in the form of ferric oxide was not dissolved. This result indicated that the zinc sulfate was completely dissolved in water and that the ferric oxide remained in the mixed residue.

CONCLUSION

The zinc ferrite, zinc oxide, zinc sulfide, and zinc silicate in the mixed residue were effectively transformed into zinc sulfate by roasting with ferric sulfate. The proportion of zinc sulfate in the mixed residue reached 90.9% after roasting at 640°C for 30 min with a ferric sulfate/residue ratio of 0.05. Water leaching was adequate for extracting zinc from the mixed, roasted residues. The zinc sulfate in the roasted residue could be completely dissolved in water, and the undesired simultaneous recovery rate of iron was only 0.13% when leaching at 25°C for 20 min with a liquid/solid ratio of 10. Therefore, the leaching liquor could be directly used for recovering zinc. This study provides useful information for separating zinc from iron and for obtaining extremely high zinc recovery rates from residues in the zinc smelting industry.

ACKNOWLEDGEMENTS

The authors gratefully acknowledge the teachers and senior fellow apprentices who helped conduct the experiments. In addition, the authors would like to thank the National High Technology Research and Development Program of China (2011AA061001), the Key Project of Science and Technology of Hunan Province, China (2012FJ1010 and2014FJ1011), and the National Natural Science Foundation of China (51474247) for supporting this study.

REFERENCES

1. M.K. Jha, V. Kumar, and R.J. Singh, *Resour. Conserv. Recycl.* 33, 1 (2001).
2. M.D. Turan, H.S. Altundoğan, and F. Tümen, *Hydrometallurgy* 75, 169 (2004).
3. A.V. Beşe, N. Borulu, M. Çopur, S. Çolak, and O.N. Ata, *Chem. Eng. J.* 162, 718 (2010).
4. D. Kuchar, T. Fukuta, M.S. Onyango, and H. Matsuda, *J. Hazard. Mater.* 137, 185 (2006).
5. P.C. Holloway, T.H. Etsell, and A.L. Murland, *Metall. Mater. Trans. B* 38, 781 (2007).
6. P.C. Holloway, T.H. Etsell, and A.L. Murland, *Metall. Mater. Trans. B* 38, 793 (2007).
7. M. Li, B. Peng, L. Chai, N. Peng, H. Yan, and D. Hou, *J. Hazard. Mater.* 237–238, 323 (2012).
8. N. Peng, B. Peng, L.-Y. Chai, M. Li, J.-M. Wang, H. Yan, and Y. Yuan, *Miner. Eng.* 35, 57 (2012).
9. H. Yan, L.-Y. Chai, B. Peng, M. Li, N. Peng, and D.-K. Hou, *Miner. Eng.* 55, 103 (2014).
10. H. Xu, C. Wei, C. Li, G. Fan, Z. Deng, M. Li, and X. Li, *Hydrometallurgy* 105, 186 (2010).
11. C. Li, F. Xie, Y. Ma, T. Cai, H. Li, Z. Huang, and G. Yuan, *J. Hazard. Mater.* 178, 823 (2010).
12. Q. Liu, Y. Zhao, and G. Zhao, *Hydrometallurgy* 110, 79 (2011).
13. M. Soylak, M. Tuzen, A.S. Souza, M.D.G.A. Korn, and S.L.C. Ferreira, *J. Hazard. Mater.* 149, 264 (2007).
14. E. Vahidi, F. Rashchi, and D. Moradkhani, *Miner. Eng.* 22, 204 (2009).
15. Z. Zhu and C.Y. Cheng, *Miner. Eng.* 39, 117 (2012).
16. J.L. Huisman, G. Schouten, and C. Schultz, *Hydrometallurgy* 83, 106 (2006).
17. A. Ruşen, A.S. Sunkar, and Y.A. Topkaya, *Hydrometallurgy* 93, 45 (2008).
18. S. Nagib and K. Inoue, *Hydrometallurgy* 56, 269 (2000).
19. J. Frenay, *Hydrometallurgy* 15, 243 (1985).
20. R. Raghavan, P.K. Mohanan, and S.C. Patnaik, *Hydrometallurgy* 48, 225 (1998).
21. R. Raghavan, P.K. Mohanan, and S.R. Swarnkar, *Hydrometallurgy* 58, 113 (2000).
22. Z.-H. Guo, F.-K. Pan, X.-Y. Xiao, L. Zhang, and K.-Q. Jiang, *Trans. Nonferr. Met. Soc. China* 20, 2000 (2010).
23. N. Leclerc, E. Meux, and J.-M. Lecuire, *J. Hazard. Mater.* 91, 257 (2002).
24. C. Drouet and A. Navrotsky, *Geochim. Cosmochim. Acta* 67, 2063 (2003).
25. J. Li, R.S.C. Smart, R.C. Schumann, A.R. Gerson, and G. Levay, *Sci. Total Environ.* 373, 391 (2007).
26. H.S. Altundoğan and F. Tümen, *Hydrometallurgy* 44, 261 (1997).
27. Y. Zhang, X. Yu, and X. Li, *Hydrometallurgy* 109, 211 (2011).